



Research Report

Direct Synthesis of Organic Compounds from CO₂, Water and Sunlight

Tsutomu Kajino, Takeshi Morikawa, Shunsuke Sato, Takeo Arai, Tomiko M. Suzuki, Keiko Uemura, Ken-ichi Yamanaka, Shu Saeki and Hiromitsu Tanaka

Report received on Apr. 27, 2012

■ABSTRACT■ We developed a new hybrid photocatalyst for CO₂ reduction, composed of a semiconductor and a metal complex. In the hybrid photocatalyst, ΔG between the E_{CBM} of the semiconductor and the CO₂ reduction potential of the complex is an essential factor for realizing high photocatalytic activity. On the basis of this concept, the hybrid photocatalyst InP/Ru-complex, which functions in aqueous media, was developed. The photoreduction of CO₂ to formate using water as an electron donor and a proton source was successfully achieved as a Z-scheme system by functionally conjugating the InP/Ru-complex photocatalyst for CO₂ reduction with a TiO₂ photocatalyst for water oxidation. The conversion efficiency from solar energy to chemical energy was ca. 0.04%, which approaches that for photosynthesis in a plant. This system can be applied to many other inorganic semiconductors and metal-complex catalysts. Therefore, the efficiency and reaction selectivity can be enhanced by optimization of the electron transfer process including the energy-band configurations, conjugation conformations, and catalyst structures. This electrical-bias-free reaction is a huge leap forward for future practical applications of artificial photosynthesis under solar irradiation to produce organic species such as alcohols, hydrocarbons, and syngas, which are useful as alternative fuels or carbon resources.

■KEYWORDS■ Solar Fuel, Photocatalyst, Semiconductor, Metal-complex, Artificial Photosynthesis, CO₂, Formic Acid

1. Preface

Developing a system for production of organic chemicals by reduction of carbon dioxide (CO₂) is increasingly becoming an important research topic that addresses both global warming and fossil fuel shortages. Among renewable energy resources, solar energy is by far the largest exploitable resource, providing more energy per hour to Earth than the total energy consumed by humans in one year. Success in CO₂ reduction by solar energy utilizing water (H₂O) as both an electron donor and a proton source leads to a system of artificial photosynthetic production of useful organic chemicals, which is an especially attractive approach to store solar energy in the form of chemical bonds.

We have successfully constructed a system mimicking natural photosynthesis utilizing a new photocatalyst composed of a semiconductor and a metal complex, which produces formic acid from CO₂ and H₂O under sunlight.

2. Past Research on Photocatalysts for CO₂ Reduction Reaction

In regard to solar CO₂ reduction, semiconductor photocatalysts such as TiO₂ and SiC are well-known to reduce CO₂.⁽¹⁾ However, in aqueous solutions they suffer from low quantum efficiencies owing to the preferential H₂ production and low selectivity for the carbon species produced. The merit of semiconductor photocatalysis lies in the fact that such materials produce H₂ and O₂ by splitting water.⁽²⁾ In other words, semiconductor photocatalysts are able to utilize H₂O as an electron donor to compensate for a hole in the photoexcited state, which is the reason why photocatalytic H₂ production with semiconductor photocatalysts is considered to be feasible. In contrast, it is generally thought that photocatalytic CO₂ reduction yielding useful chemicals is more difficult than H₂ production. Metal complexes, however, are also well-known photocatalysts for CO₂ reduction.⁽³⁻⁶⁾ Their quantum efficiencies and product selectivities are quite high. For example, the quantum yield of conversion of CO₂ to CO ranges up to 38% with fac-

$[\text{Re}(\text{bpy})(\text{CO})_3\{\text{P}(\text{OEt})_3\}]^+$ (bpy: 2,2'-bipyridine),^(3b) and only a very small amount of hydrogen and no formic acid are produced even in the presence of water. However, to ensure a successful photocatalytic CO_2 reduction with metal complexes, a suitable electron donor for the photocatalyst in the photoexcited state must be found. Currently, such photocatalysts require electron donors such as triethanolamine (TEOA), because there are no complex photocatalysts that are able to extract electrons from H_2O .

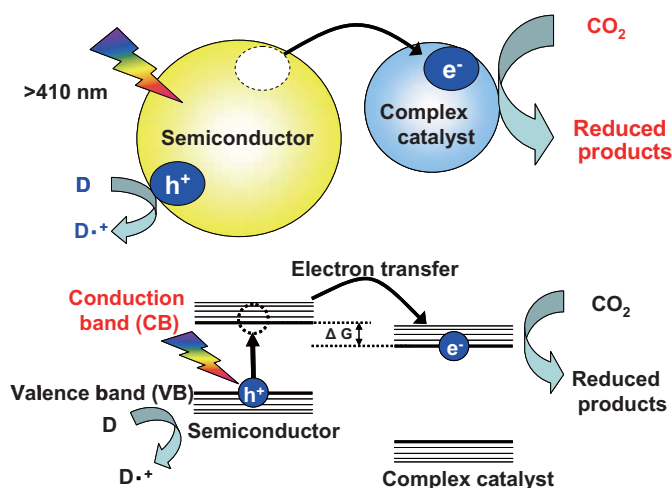
3. Proof of Concept for Selective CO_2 Reduction Using a Semiconductor/metal-complex Hybrid

3.1 Concept for a Semiconductor/metal-complex Hybrid Photocatalyst

The development of photocatalysts that can selectively reduce CO_2 to organic substances in water is crucial to realize artificial photosynthesis. We considered that useful organic chemicals could be obtained with high selectivity and activity in aqueous solutions by combining photoactive semiconductors with metal complexes capable of catalytically reducing CO_2 . A Z-scheme system, which makes use of heterogeneous semiconductors with different band energy potentials for producing H_2 and O_2 from H_2O ,⁽⁷⁾ will be applicable to a hybrid system for CO_2 reduction. There is, however, a technical barrier to realize this type of photocatalytic CO_2 reduction with a hybrid system. It is essential that photoexcited electrons are transferred from the conduction band (CB) of the semiconductor to the metal complex to promote selective CO_2 reduction on the complex (Scheme 1). There have been no reports of photocatalytic reduction of CO_2 by such a mechanism.

To develop a hybrid photocatalyst for CO_2 reduction, we used the complex catalyst $[\text{Ru}(\text{dcbpy})_2(\text{CO})_2]^{2+}(\text{Cl}^-)_2$ ($[\text{Ru-dcbpy}]$) (Fig. 1), which can act as an electrocatalyst for CO_2 reduction.⁽⁶⁾ The CO_2 reduction potential over $[\text{Ru-dcbpy}]$ was measured by cyclic voltammetry which is obtained in MeCN and purged with CO_2 . The threshold potentials giving large second peaks originating from the secondary electron injection into CO_2 through $[\text{Ru-dcbpy}]$ were at ca. -0.8 V (vs. normal hydrogen electrode, NHE). Therefore, the potential of CB minimum (E_{CBM}) of the semiconductor should be much more negative than the reduction potential for CO_2 over $[\text{Ru-dcbpy}]$.⁽⁸⁾ For the present purpose, we

developed N- Ta_2O_5 powder with an orthorhombic Ta_2O_5 crystalline structure that absorbs visible light at wavelengths shorter than 520 nm.⁽⁹⁾ Nitrogen doping not only causes a red shift at the absorption edge of Ta_2O_5 by 200 nm (Ta_2O_5 absorbs UV light of < 320 nm) as was found for N-doped TiO_2 ,⁽¹⁰⁾ but it also provides p-type conductivity as in N-doped ZnO , as reported previously.⁽¹¹⁾ Since the average crystal size estimated from the full width at half maximum (FWHM) of the diffraction peak using the Scherrer equation was around 20 nm, the band-gap widening arising from the quantum size effect was negligible. The ionization potential, or the valence band maximum (E_{VBM}), of N- Ta_2O_5 was estimated to be about +1.1 V (vs. NHE) by photoelectron spectroscopy in air



Scheme 1 Schematic illustration and energy diagram of the semiconductor/metal-complex photocatalyst for CO_2 reduction.

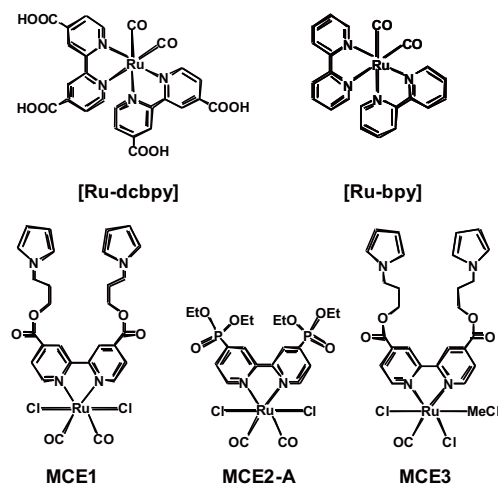


Fig. 1 Structures of the metal catalyst complexes.

(PESA).⁽¹²⁾ It is favorable that the band potential of Ta₂O₅ was shifted to a more negative position with nitrogen doping. The resulting E_{CBM} was calculated to be -1.3 V (vs. NHE), so the ΔG values (energy difference between the E_{CBM} of a semiconductor and the CO₂ reduction potential in a metal complex) between the E_{CBM} of N-Ta₂O₅ and the reduction potential of Ru complexes were -0.5 V.

3.2 CO₂ Reduction over [Ru-dcbpy]/N-Ta₂O₅ in MeCN under Visible Light

Visible light passing through UV and IR cut filters installed in a Xe lamp was used to irradiate 8 mL test tubes containing the photocatalysts (0.05 mm metal complex and/or 5 mg semiconductor) and 4 mL MeCN/TEOA (5:1 v/v) purged with CO₂. In this experiment, we used MeCN as a solvent taking into account the stable CO₂ reduction of [Ru(bpy)₂(CO)₂]²⁺(Cl)₂[Ru-bpy] (Fig. 1). The catalysts examined were [Ru-bpy], N-Ta₂O₅, and [Ru-dcbpy]/N-Ta₂O₅. The amounts of the main photocatalytic product (HCOOH) as a function of irradiation time under visible light are shown in Fig. 2. It became clear that [Ru-dcbpy]/N-Ta₂O₅ acted as a photocatalyst for CO₂ reduction. However,

[Ru-bpy] and N-Ta₂O₅ did not show photocatalytic activity for CO₂ reduction. Only [Ru-dcbpy]/N-Ta₂O₅ exhibited a significant photocatalytic reaction rate for HCOOH generation, showing a turnover number (TN_{HCOOH}) per metal complex of 89. H₂ and CO were also detected, but the selectivity for HCOOH formation was more than 75% before the saturation of TN_{HCOOH} . It is noteworthy that the present TN of 89 obtained using the semiconductor-complex hybrid is comparable to the highest TN of 240 for the conversion of CO₂ into CO using a rhenium complex photocatalyst.^(5a) We confirmed that the amount of HCOOH produced increased linearly with the amount of [Ru-dcbpy]/N-Ta₂O₅ up to 50 mg in the same photoreactor. The photocatalytic rate of HCOOH generation using 50 mg of photocatalyst was calculated to be 3.5 mmol/h. This rate was found to be comparable to that of photocatalytic H₂ production using a semiconductor photocatalyst, which is also supported by the high quantum yield of the present CO₂ reduction. Figure 3 shows an action spectrum of the quantum yield of HCOOH generation on [Ru-dcbpy]/N-Ta₂O₅. The measured quantum yield of HCOOH formation (Φ_{HCOOH}) was 1.9% at 405 nm. It was found that Φ_{HCOOH} was strongly dependent on the optical absorption of N-Ta₂O₅. Because [Ru-bpy] does

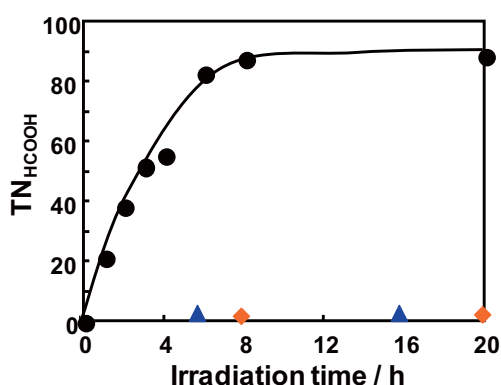


Fig. 2 Turnover number (TN) for HCOOH formation from CO₂ as a function of irradiation time. Solutions were irradiated using a Xe lamp with filters producing light in the range of $410 \leq \lambda \leq 750$ nm. The concentrations of the photocatalysts were 0.05 mM and 5 mg for the Ru-complexes and semiconductors, respectively, in a CO₂ saturated MeCN/TEOA (5:1) solution. The catalysts used were [Ru-bpy] (blue triangles), N-Ta₂O₅ (orange diamonds), and [Ru-dcbpy]/N-Ta₂O₅ (black circles).

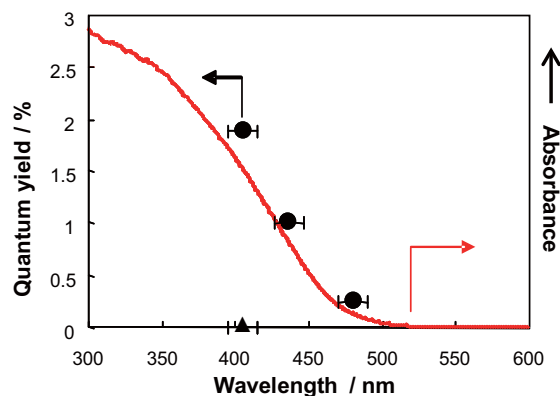


Fig. 3 Quantum efficiency (filled circles or triangle) at HCOOH generation and optical absorption of N-Ta₂O₅ (red line) plotted as a function of wavelength of the incident light. 4 mL of MeCN-TEOA (5:1 v/v) solutions containing 20 mg of [Ru-dcbpy]/N-Ta₂O₅ (circles) or 0.01 mM of [Ru-dcbpy] (triangle) were irradiated under CO₂ with 405 nm (2.06×10^{-8} einstein s⁻¹), 435 nm (4.58×10^{-8} einstein s⁻¹) and 480 nm (4.89×10^{-8} einstein s⁻¹) monochromatic light, respectively.

not act as a photocatalyst, but functions as an electrocatalyst for CO₂ reduction, it can be concluded that photocatalytic CO₂ reduction takes place owing to electron transfer from N-Ta₂O₅ in the excited state to the Ru complex. Our recent research also clarified that a direct assembly synthesis of the Ru-complex onto the surface of N-Ta₂O₅, which facilitates its production, is applicable and that a Ru-complex anchored onto N-Ta₂O₅ by phosphonate exhibited excellent photoconversion activity of CO₂ to formic acid relative to [Ru-dcbpy]/N-Ta₂O₅ under visible-light irradiation with respect to the reaction rate and stability.⁽¹³⁾

3.3 Charge Carrier Dynamics in N-Ta₂O₅/[Ru(dcbpy)₂(CO)₂]²⁺

Understanding the photoinduced electron-transfer process and the reaction mechanism of semiconductor/metal-complex hybrid photocatalysts is essential for the detailed design of the system. Hence, the excited-state dynamics of [Ru-dcbpy]/N-Ta₂O₅ were investigated by time-resolved emission measurements.⁽¹⁴⁾

First, it was found that, as a primary process, a structural change took place in the Ru complex adsorbed onto N-Ta₂O₅, which changed from [Ru(dcbpy)₂(CO)₂]²⁺ to [Ru(dcbpy)₂(CO)(COOH)]⁺ as observed by FTIR. [Ru(dcbpy)₂(CO)(COOH)]⁺ is the final form that functions as a CO₂ reduction catalyst in the [Ru-dcbpy]/N-Ta₂O₅ system. As for N-Ta₂O₅, it had already been reported that two distinct levels (shallow and deep defect levels) were generated due to a heavy doping of N in Ta₂O₅.⁽¹⁵⁾ Visible excitation at 400 nm (Ta_{5d} ← N_{2p} transition) revealed a fast trapping process from shallow defect sites to deep defect sites with a time constant of 24 ± 1 ps in N-Ta₂O₅ powder (Fig. 4). In [Ru-dcbpy]/N-Ta₂O₅, ultrafast electron transfer from the shallow defect sites of N-Ta₂O₅ to the adsorbed Ru complex occurred with a time constant of 12 ± 1 ps. The values of the rate constant (*k*_{et}) and quantum yield (*Φ*_{et}) of the electron transfer process were estimated to be 4.2 × 10¹⁰ s⁻¹ and 0.50, respectively. No electron injection from the Ru complex to N-Ta₂O₅ was observed upon selective excitation of the Ru complex. Hence the primary photochemical process for the CO₂ reduction photocatalyst [Ru-dcbpy]/N-Ta₂O₅ was explained based on the competition between ultrafast electron transfer from N-Ta₂O₅ to [Ru(dcbpy)₂(CO)(COOH)]⁺, and the carrier trapping processes in N-Ta₂O₅. On the basis of the driving force

of electron transfer from the shallow defect sites to the HOMO ($\Delta G \approx -0.4$), this *k*_{et} value of [Ru-dcbpy]/N-Ta₂O₅ is comparable with that of CdSe quantum dots with adsorbed Re(CO)₃Cl(dcbpy). The exciton dissociation half-times of CdSe quantum dots with different first exciton oxidation potentials were about 2.3 ps ($\Delta G = -0.59$ eV), 55.5 ps ($\Delta G = -0.41$ eV), and 1 ns ($\Delta G = -0.3$ eV).⁽¹⁶⁾ These facts strongly suggest that ΔG is one of the essential factors that facilitates CO₂ reduction over metal-complexes of semiconductor/complex hybrid photocatalysts.

3.4 Summary of the Proof of Concept for Selective CO₂ Reduction Using Semiconductor/metal-complex Hybrid

Isotope tracer analyses using ¹³CO₂, D₂O and CD₃CN revealed that the carbon source of HCOOH is gaseous CO₂, and TEOA is necessary not only as an electron donor, but also as a proton source for HCOOH formation. This general concept for the semiconductor/complex hybrid photocatalyst is applicable to many non-photoactive complex electrocatalysts and also to hundreds of photoactive semiconductor. The highly active photocatalyst could be realized using a semiconductor with an oxidative power strong enough to extract electrons from H₂O in aqueous solutions and a complex with high CO₂ reduction selectivity.

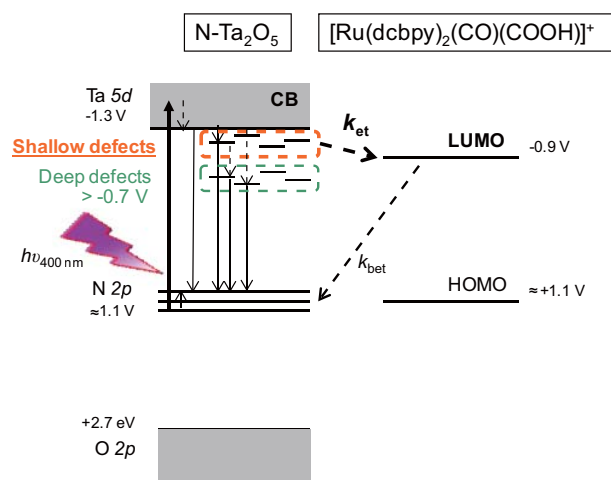


Fig. 4 Schematic illustration of the energy diagram of N-Ta₂O₅ and [Ru(dcbpy)₂(CO)(COOH)]⁺. All energy levels were normalized vs. NHE.

4. A Hybrid Photocatalyst for CO₂ Reduction Active in Aqueous Media

4.1 Synthesis and Catalytic Properties of the Hybrid Photocatalyst

To reduce CO₂ using H₂O as electron donor, CO₂ photoreduction to HCOOH must be achieved in water. The [Ru-dcbpy]/N-Ta₂O₅ hybrid photocatalyst mentioned above can operate only in an organic solvent, not in water. We applied the concept of the hybrid photocatalyst to develop a photocatalyst for CO₂ reduction that would be active under aqueous conditions. Ruthenium complex polymer (RCP) ([Ru(L-L)(CO)₂]_n, L-L: a diimine ligand) catalyst reported by Deronzier et al.⁽¹⁷⁾ and p-type InP (zinc doped indium phosphide wafer purchased from Sumitomo Electric Industries, Ltd.) were used as complex catalyst and semiconductor, respectively, to prepare the hybrid photocatalyst for CO₂ reduction. The surface of InP wafer was modified with [Ru{4,4'-di(1H-pyrrolyl-3-propyl carbonate)-2,2'-bipyridine}(CO)₂Cl₂] (MCE1) (Fig. 1) by electropolymerization, referring to the method reported by Deronzier et al.⁽¹⁷⁾ Linear sweep voltammograms of MCE1 modified InP electrode (InP/MCE1) measured in dark or under visible light irradiation with CO₂ or Ar bubbling are shown in Fig. 5. A clear CO₂ reduction current in dark was observed at less than ca. -0.8 V (vs. Ag/AgCl), which was confirmed to be equal to that observed over MCE1 on a glassy carbon electrode (MCE1/carbon).

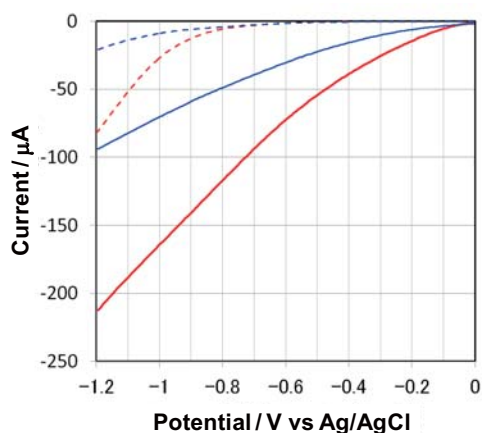


Fig. 5 Linear-sweep voltammetry of an InP/MCE1 photocatalyst under dark (dotted line) or visible-light irradiation ($400 < \lambda < 800$ nm) (solid line) with Ar (blue) or CO₂ (red) bubbling, respectively.

On the other hand, the CO₂ reduction photocurrent under visible light irradiation was observed at less than 0 V, which corresponds to the position of the valence band maximum (E_{VBM}) of InP. The position of the E_{CBM} of p-InP-Zn was calculated to be approximately -1.35 V (vs. Ag/AgCl) by subtracting the bandgap value of InP (1.35 eV),⁽¹⁸⁾ from E_{VBM} . The E_{CBM} was found to be sufficiently more negative than the potential reduction of CO₂ (-0.8 V vs. Ag/AgCl). These results suggest that in the InP/MCE1 hybrid photocatalyst, InP can lower the level of external electrical bias for reducing CO₂ down to E_{VBM} . In the chronoamperometry measurements at -0.6 V (vs. Ag/AgCl) in pure water, 3.01 $\mu\text{mol}/\text{cm}^2$ of HCOO⁻, which was confirmed to be the main product and identified as m/z 45 by ion-chromatography-time-of-flight mass-spectroscopy (IC-TOFMS), was produced over InP/MCE1 under visible light irradiation for 3 h with CO₂ bubbling.

The turnover number for formate formation per Ru-complex was over 12, suggesting a catalytic reaction. On the contrary, the total charge over the unmodified InP electrode was very low compared with that of InP/MCE1, and no HCOO⁻ was produced. HCOO⁻ was observed only over the InP/MCE1 electrode in the presence of both visible light and CO₂. These results suggest that RCP can accept photoexcited electrons from InP and reduce CO₂ efficiently.

4.2 Improvement of the Catalytic Activity for CO₂ Reduction

We attempted to introduce another Ru-complex containing an anchor ligand into MCE with the aim of improving the electron transfer from semiconductor to MCE. The following Ru complexes were synthesized: [Ru(4,4'-diphosphate ethyl-2,2'-bipyridine)(CO)₂Cl₂] (MCE2-A) and [Ru{4,4'-di(1H-pyrrolyl-3-propyl carbonate)-2,2'-bipyridine}(CO)(MeCN)Cl₂] (MCE3) (Fig. 1). MCE2-A has 4,4'-diphosphate ethyl-2,2'-bipyridine anchor ligands. MCE3 has the same activity for CO₂ reduction as MCE1, but is more stable to use than MCE1.

Figure 6 shows successive formate generation from CO₂ over the InP/[MCE]s performed using a three-electrode configuration in pure water under visible light irradiation. The applied potential (-0.4 V vs. Ag/AgCl) was set more positive than E_{red} (-0.8 V vs. Ag/AgCl) and was approximately equal to the E_{CBM} of anatase TiO₂ (described later). All of the InP/[MCE]s

could reduce CO_2 to formate, but InP showed almost no activity towards formate formation. InP/MCE3 (chemical-polymerized) exhibited a higher photocatalytic activity than InP/MCE1 (electropolymerized). Furthermore, InP/[MCE2-A+MCE3] exhibited the highest photocatalytic reaction rate for formate generation.

An accelerated electron transfer from the photoexcited semiconductor to a complex anchored to the surface of a semiconductor was reported on the CdSe/[Re(dcbpy)(CO)₃Cl] system⁽²⁰⁾ and the N-Ta₂O₅/[Ru(dcbpy)₂(CO)₂]²⁺ photocatalyst.⁽¹⁴⁾ MCE2-A has the ligand anchored onto the phosphide, so that MCE2-A can link tightly with the surface of InP.⁽¹⁹⁾ One possible reason for the enhanced reaction rate for the mixture of MCE2-A and MCE3 may be due to accelerated electron transfer from the photoexcited InP to [MCE2-A+MCE3]. Furthermore, electron-transfer from MCE2-A to MCE3 is presumed to occur in the mixture, because of the following:

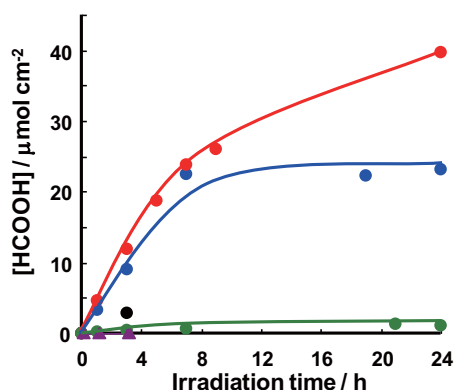


Fig. 6 Photoelectrocatalytic HCOOH formation from CO_2 as a function of irradiation time over InP/[MCE]s. Photoelectrochemical CO_2 reduction was performed in pure water using a three-electrode configuration. The photocathode (hybrid InP/[MCE]s photocatalyst), glassy carbon and Ag/AgCl were used as the working, counter and reference electrodes, respectively. A Pyrex glass cell was used as a reactor, and a xenon light source equipped with an optical filter ($\lambda > 400$ nm) and a cold mirror was used to irradiate visible light (ca. 70 SUN). The applied potential was -0.4 V (vs. Ag/AgCl). The InP/[MCE] hybrid photocatalysts used were InP (purple), electropolymerized InP/[MCE1] (black), chemical-polymerized InP/[MCE2-A] (green), chemical-polymerized InP/[MCE3] (blue) and chemical-polymerized InP/[MCE2-A+MCE3] (red).

(i) InP/MCE2-A exhibited a lower efficiency for formate formation (EFF) even with a higher photocurrent than InP/MCE3, which indicates that InP/MCE2-A has less selectivity for formate generation (Fig. 6).

(ii) InP/[MCE2-A+MCE3] had a higher rate for formate generation than InP/MCE3, although the EFF was almost identical (ca. 80%), which indicates that a larger reaction photocurrent was generated in InP/[MCE2-A+MCE3] than in InP/[MCE4].

These results indicate that MCE2-A could play a more important role as an electron transfer facilitator to improve CO_2 reduction over MCE3 in InP/[MCE2-A+MCE3], rather than as a catalyst for formate generation. To clear the charge carrier dynamics for the hybrid photocatalyst InP/[MCE2-A+MCE3], diffuse-reflectance transient spectroscopic analyses of this type of fast electron transfer process in the present system are now underway. The highest formate generation rate over InP/[MCE2-A+MCE3] was approximately seven times that over InP/MCE1. Consequently, InP/[MCE2-A+MCE3] was selected as the photocatalyst for CO_2 reduction.

5. Selective CO_2 Photoreduction to Formate Conjugated with H_2O Oxidation

It is reported that heterogeneous semiconductors with different band-energy potentials for producing H_2 and O_2 from H_2O have been applied to systems for photocatalytic water splitting.⁽²¹⁾ The hybrid photocatalyst InP/[MCE2-A+MCE3] can selectively reduce CO_2 to formate in water. By combination with a photocatalyst capable of water oxidation such as a Z-scheme (or two-step photoexcitation) system, it can be expected that this will facilitate the development of a photo-utilizing system of CO_2 that uses H_2O as both an electron and proton source.

In order to realize a system to selectively reduce CO_2 with no external electrical bias, using H_2O as an electron donor, we developed the Z-scheme system (Fig. 7) by functionally combining InP/[MCE2-A+MCE3] with a photocatalyst for water oxidation. The E_{VBM} of the photocatalyst for water oxidation must be more positive than the potential for water oxidation (theoretically 1.23 V vs. NHE). Furthermore, the E_{CBM} of the photocatalyst for water oxidation should be more negative than the E_{VBM} of the photocatalyst for CO_2 reduction to ensure electron transfer from the photoanode to the photocathode with no external

electrical bias. In this work, anatase titanium dioxide on a conducting glass (TiO_2) was used as the photocatalyst for water oxidation, taking into account the E_{CBM} of TiO_2 , the E_{VBM} of $\text{InP}/[\text{MCE2-A}+\text{MCE3}]$, and the oxygen generation ability for oxidizing water.⁽²²⁾ The potential difference of the E_{CBM} of TiO_2 from the E_{VBM} of InP was estimated to be -0.5 V. Hence a successful electron transfer between two photocatalysts with no external electrical bias can be facilitated due to this potential difference.⁽²³⁾ The reduction of CO_2 conjugated with water oxidation was performed using a two-electrode configuration (Fig. 8). CO_2 reduction photocatalyst $\text{InP}/[\text{MCE2-A}+\text{MCE3}]$ ($20 \times 15 \text{ mm}^2$, black-colored) and water oxidation photocatalyst TiO_2 ($20 \times 15 \text{ mm}^2$, translucent) were used. A two-compartment Pyrex cell separated with a proton exchange membrane was used

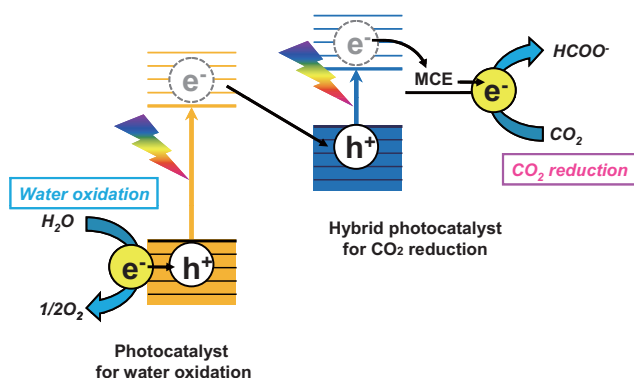


Fig. 7 Schematic energy diagram of the total reaction of the Z-scheme system for CO_2 reduction.

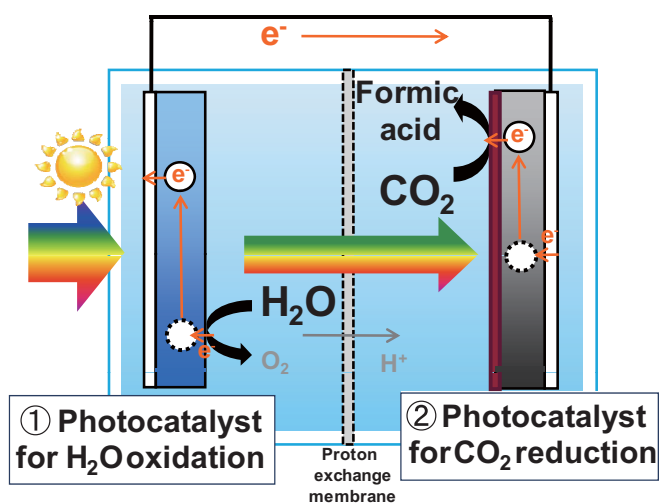


Fig. 8 Schematic illustration of the tandem-cell reactor.

as the reactor to prevent re-oxidation of the formate over TiO_2 . A 10 mM NaHCO_3 solution was used as a suitable electrolyte solution for $\text{InP}/[\text{MCE2-A}+\text{MCE3}]$, and it also accelerated catalytic oxygen generation over the TiO_2 photoanode.⁽²⁴⁾ A solar simulator equipped with an air mass 1.5 (AM 1.5) filter was used as the light source with the intensity adjusted to 1 SUN. The irradiation area was $10 \times 10 \text{ mm}^2$. Light was irradiated from the TiO_2/Pt side, and $\text{InP}/[\text{MCE2-A}+\text{MCE3}]$ was irradiated with light transmitted through the TiO_2/Pt photocatalyst electrode and proton exchange membrane. No external electrical bias was applied between the two photocatalysts. Stable photocatalytic production of formate was observed for 24 h under irradiation (1 SUN) with CO_2 bubbling (Fig. 9). The turnover number of HCOOH was over 17 at 24 h and larger values would be expected with further irradiation. Even though H_2 and CO were also detected, the value of EFF reached approximately 70%, which was similar to that observed over $\text{InP}/[\text{MCE2-A}+\text{MCE3}]$ in the three-electrode

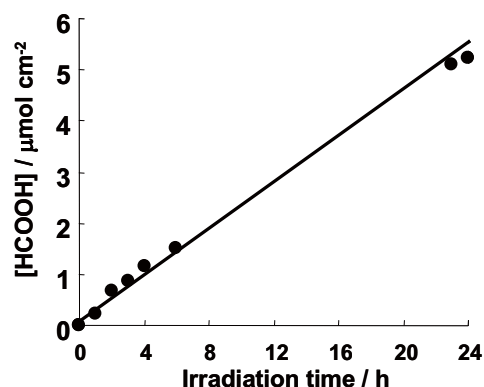
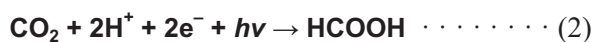
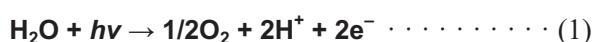


Fig. 9 Photocatalytic HCOOH formation from CO_2 as a function of irradiation time using $\text{InP}/[\text{MCE2-A}+\text{MCE3}]$ conjugated with TiO_2/Pt . CO_2 reduction was performed using a two-electrode configuration with no external electrical bias in 10 mM NaHCO_3 solution (see Fig. 8). $\text{InP}/[\text{MCE2-A}+\text{MCE3}]$ and TiO_2/Pt were used as photocatalysts for CO_2 reduction and water oxidation, respectively. A two compartment Pyrex cell separated by a proton exchange membrane (Nafion117, DuPont) was used as the reactor. A solar simulator, in which the intensity was adjusted to 1 SUN (AM1.5), was used as the light source. Light was irradiated from the TiO_2/Pt side, and $\text{InP}/[\text{MCE2-A}+\text{MCE3}]$ was irradiated with light transmitted through the translucent TiO_2/Pt and proton exchange membrane. The irradiation area was $10 \times 10 \text{ mm}^2$.

configuration. The conversion efficiency from solar energy to chemical energy was ca. 0.04%, which was calculated by dividing the combustion heat of formic acid generated by the integrated energy of the irradiated solar simulating light (AM1.5). This value is one fifth of 0.2%, which is the solar conversion efficiency of switchgrass, a promising crop for biomass fuel.⁽²⁵⁾ From isotope tracer analysis using ¹³CO₂ and D₂O, the carbon and proton source of the formate was determined to be derived from CO₂ and H₂O, respectively. A negligible amount of H¹²COO⁻ was observed for ¹³CO₂, even in the presence of H¹²CO₃⁻. These results indicate that the formate detected in the reaction was mainly produced from the CO₂ molecules in the solution, not from carbonate ions. Furthermore, ¹⁸O₂ was detected by gas chromatography-mass spectrometry (GC-MS) in the gas phase at the oxidation site after reaction using an aqueous solution containing 25% H₂¹⁸O. These results verified that CO₂ was reduced to formate by electrons extracted from H₂O during the oxidation process to O₂, and that protons also originated from H₂O (Eqs. 1 and 2).



6. Conclusion

We constructed a new concept for a CO₂ reduction photocatalyst: a hybrid of a semiconductor and a metal complex. In the hybrid photocatalyst, ΔG between the E_{CBM} of the semiconductor and the CO₂ reduction potential of the complex is an essential factor for realizing efficient photocatalytic activity. On the basis of this concept, the hybrid photocatalyst InP/Ru-complex, which functions in aqueous media, was developed. The photoreduction of CO₂ to formate using water as both an electron donor and a proton source was successfully achieved as a Z-scheme system by functionally conjugating the InP/Ru-complex photocatalyst for CO₂ reduction with a TiO₂ photocatalyst for water oxidation. The conversion efficiency from solar energy to chemical energy was ca. 0.04%, which approaches that for photosynthesis in a plant. This system can be applied to many other inorganic semiconductors and MCEs. Therefore, the efficiency and reaction selectivity can be enhanced by optimization of the electron transfer process including

the energy-band configurations, conjugation conformations, and catalyst structures. This electrical-bias-free reaction is a huge leap forward for future practical applications of artificial photosynthesis under solar irradiation to produce organic species such as alcohols, hydrocarbons, and syngas, which are useful as alternative fuels or carbon resources.

References

- (1) (a) Halmann, M., *Nature*, Vol.275 (1978), p.115; (b) Inoue, T., Fujishima, A., Konishi, S. and Honda, K., *Nature*, Vol.277 (1979), p.637.
- (2) (a) Sato, S. and White, J. M., *Chem. Phys. Lett.*, Vol.72 (1980), p.83; (b) Kato, H., Asakura, K. and Kudo, A., *J. Am. Chem. Soc.*, Vol.125 (2003), p.3082; (c) Maeda, K., Teramura, K., Lu, D., Takata, T., Saito, N., Inoue, Y. and Domen, K., *Nature*, Vol.440 (2006), p.295.
- (3) (a) Hawecker, J., Lehn, J.-M., Ziessel, R., *Helv. Chim. Acta*, Vol.69 (1986), p.1990; (b) Hori, H., Johnson, F. P. A., Koike, K., Ishitani, O. and Ibusuki, T., *J. Photochem. Photobiol. A*, Vol.96 (1996), p.171.
- (4) Matsuoka, S., Yamamoto, K., Ogata, T., Kusaba, M., Nakashima, N., Fujita, E. and Yanagida, S., *J. Am. Chem. Soc.*, Vol.115 (1993), p.601.
- (5) (a) Gholamkhash, B., Mametuka, H., Koike, K., Tanabe, T., Furue, M. and Ishitani, O., *Inorg. Chem.*, Vol.44 (2005), p.2326; (b) Sato, S., Koike, K. Inoue, H. and Ishitani, O., *Photochem. Photobiol. Sci.*, Vol.6 (2007), p.451.
- (6) (a) Ishida, H., Terada, T., Tanaka, K. and Tanaka, T., *Organometallics*, Vol.6 (1990), p.181; (b) Tanaka, K., *Bull. Chem. Soc. Jpn.*, Vol.71 (1998), p.17.
- (7) (a) Sayama, K., Mukasa, K., Abe, R., Abe, Y. and Arakawa, H., *J. Photochem. Photobiol. A*, Vol.148 (2002), p.71; (b) Kato, H., Sasaki, Y., Iwase, A. and Kudo, A., *Bull. Chem. Soc. Jpn.*, Vol.80 (2007), p.2457.
- (8) Sato, S., Morikawa, T., Saeki, S., Kajino, T. and Motohiro, T., *Angew. Chem., Int. Ed.*, Vol.49 (2010), p.5101.
- (9) Morikawa, T., Saeki, S., Suzuki, T., Kajino, T. and Motohiro, T., *Appl. Phys. Lett.*, Vol.96 (2010), p.142111.
- (10) Asahi, R., Morikawa, T., Ohwaki, T., Aoki, K. and Taga, Y., *Science*, Vol.293 (2001), p.269.
- (11) Tsukazaki, A., Ohtomo, A., Onuma, T., Ohtani, M., Makino, T., Sumiya, M., Ohtani, K., Chichibu, S. F., Fuke, S., Segawa, Y., Ohno, H., Koinuma, H. and Kawasaki, M., *Nature Mater.*, Vol.4 (2005), p.42
- (12) Uchida, T., Mimura, T., Ohtsuka, M., Otomo, T., Ide, M., Shida, A. and Sawada, Y., *Thin Solid Films*, Vol.496 (2006), p.75
- (13) Suzuki, T. M., Tanaka, H., Morikawa, T., Iwaki, M., Sato, S., Saeki, S., Inoue, M., Kajino, T. and Motohiro, T., *Chem. Commun.*, Vol.47, No.30 (2010), pp.8673-8675.

- (14) Yamanaka, K., Sato, S., Iwaki, M., Kajino, T. and Morikawa, T., *J. Phys. Chem. C*, Vol.115 (2011), pp.18348-18353.
- (15) Shin, H., Park, S. Y., Bae, S.-T., Lee, S., Hong, K. S. and Jung, H. S., *J. Appl. Phys.*, Vol.104 (2008), pp.116108.
- (16) Huang, J., Stockwell, D., Huang, Z., Mohler, D. L. and Lian, T., *J. Am. Chem. Soc.*, Vol.130 (2008), p.5632.
- (17) (a) Chardon-Noblat, S., Deronzier, A., Zieseel, R. and Zsoldos, D., *J. Electroanal. Chem.*, Vol.444 (1998), p.253; (b) Tanaka, K., *Bull. Chem. Soc. Jpn.*, Vol.71 (1998), p.17; (c) Ramos Sende, J. A., Arana, C. R., Hernandez, L., Potts, K. T., Keshevarz-K, M. and Abruna, H. D., *Inorg. Chem.*, Vol.34 (1995), p.3339; (d) Save'ant, J.-M., *Chem. Rev.*, Vol.108 (2008), p.2348; (e) Mikkelsen, M., Jorgensen, M. and Krebs, F. C., *Energy Environ. Sci.*, Vol.3 (2010), p.43.
- (18) Parkinson, B. A. and Weaver, P. F., *Nature*, Vol.309 (1984), p.148.
- (19) Guzelian, A. A., Katari, J. E. B., Kadavanich, A. V., Banin, U., Hamad, K., Juban, E., Alivisatos, A. P., *J. Phys. Chem.*, Vol.100 (1996), p.7212.
- (20) Huang, J., Stockwell, D., Huang, Z., Mohler, D. L. and Lian, T., *J. Am. Chem. Soc.*, Vol.130 (2008), p.5632.
- (21) (a) Leygraf, C., Hendewerk, M. and Somorjai, G. A., *J. Phys. Chem.*, Vol. 86 (1982), p.4484; (b) Sayama, K., Mukasa, K., Abe, R., Abe, Y. and Arakawa, H., *Chem. Commun.*, Vol.35 (2001), p.2416.
- (22) Sato, S. and White, J. M., *Chem. Phys. Lett.*, Vol.72 (1980), p.83.
- (23) Ida, S., Yamada, K., Matsunaga, T., Hagiwara, H., Matsumoto, Y. and Ishihara, T., *J. Am. Chem. Soc.*, Vol.132 (2010), p.17343.
- (24) Sayama, K., Augustynski, J. and Arakawa, H., *Chem. Lett.*, Vol.31 (2002), p.994.
- (25) Lewandowski, I., Scurlock, J. M. O., Lindvall, E. and Christou, M., *Biomass Bioenergy*, Vol.25 (2003), p.335.

Fig. 3

Reprinted from *Angew. Chem., Int. Ed.*, Vol.49 (2010), pp.5101-5105, Sato, S., Morikawa, T., Saeki, S., Kajino, T. and Motohiro, T., Visible-light-induced Selective CO₂ Reduction Utilizing a Ruthenium Complex Electrocatalyst Linked to a p-Type Nitrogen-doped Ta₂O₅ Semiconductor, © 2010 Wiley, with permission from Wiley-VCH Verlag GmbH & Co. KGaA.

Fig. 9

Reprinted from *J. Am. Chem. Soc.*, Vol.133 (2011), pp.15240-15243, Sato, S., Arai, T., Morikawa, T., Uemura, K., Suzuki, T. M., Tanaka, H. and Kajino, T., Selective CO₂ Conversion to Formate Conjugated with H₂O Oxidation Utilizing Semiconductor/Complex Hybrid Photocatalysts, © 2011 ACS, with permission from American Chemical Society.

Tsutomu Kajino

Research Fields:

- Solar Fuel Production
- Catalytic Chemistry

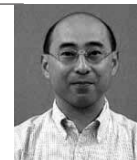
Academic Degree: Dr. Agr.

Academic Societies:

- Chemical Society of Japan
- The Society for Biotechnology, Japan

Awards:

- R&D 100 Award, 2002
- Technology Development Award of Jpn. Fine Ceram. Assoc., 2005



Takeshi Morikawa

Research Fields:

- Photocatalysis
- Semiconductor Physics

Academic Degree: Dr. Eng.

Academic Societies:

- IEEE
- The Chemical Society of Japan

Awards:

- R&D 100 Award, 1993
- Technology Development Award of Jpn. Fine Ceram. Assoc., 2003
- Award of Outstanding Papers of Ceram. Soc. Jpn., 2005
- Ceram. Soc. Jpn. Technology Award, 2006
- The Am. Ceram. Soc. Corporate Environmental Achievement Award, 2006
- The Chem. Soc. Jpn., Award for Technical Development, 2007



Shunsuke Sato

Research Fields:

- Photocatalysis
- Photochemistry of Coordination Compounds

Academic Degree: Dr. Sci.

Academic Societies:

- The Chemical Society of Japan
- The Photofunctional Complexes Research Association

Award:

- CSJ Student Presentation Award, 2005



Takeo Arai

Research Fields:

- Solar Fuels
- Photocatalysis
- Photoelectrochemistry

Academic Degree: Dr. Phi

Academic Societies:

- The Electrochemical Society of Japan
- Catalysis Society of Japan
- The Chemical Society of Japan

Award:

- Paper Award, The Electrochemical Society of Japan, 2009

**Keiko Uemura**

Research Fields:

- Solar Fuels
- Biological Engineering
- Porous Materials

**Ken-ichi Yamanaka**

Research Fields:

- Physical Chemistry
- Photochemistry
- Time-resolved Spectroscopy

Academic Degree: Dr. Sci.

Academic Societies:

- The Chemical Society of Japan
- The Japanese Photochemistry Association
- Japan Society for Molecular Science

**Tomiko M. Suzuki**

Research Field:

- Catalytic Chemistry

Academic Degree: Dr. Eng.

Academic Societies:

- American Chemical Society
- The Chemical Society of Japan
- Catalysis Society of Japan
- The Society of Polymer Science, Japan

Awards:

- Tokai Chemical Industry Association Award, 2000
- JBB Excellent Paper Award, The Society for Biotechnology, Japan, 2007
- 14th International Congress on Catalysis Pre-symposium, Best Poster Presentation Award, 2008

**Shu Saeki**

Research Field:

- Photocatalysis

Academic Degree: Dr. Eng.

Academic Society:

- The Society of Powder Technology, Japan

**Hikomitsu Tanaka**

Research Fields:

- Composite Materials
- Functional Materials

Academic Degree: Dr. Eng.

Academic Society:

- The Chemical Society of Japan

